J Mater Sci: Mater Electron (2015) 26:4722–4729
DOI 10.1007/s10854-015-2949-8

Silicon nanowires: applications in catalysis with distinctive surface property

Fan Liao[1] · Tao Wang[1] · Mingwang Shao[1]

Received: 22 January 2015 / Accepted: 13 March 2015 / Published online: 21 March 2015

Abstract Over the last few years, silicon nanowires (SiNWs) have come under intensive researches due to their electrical, optical, mechanical, thermal, and chemical properties. On account of their large surface-to-volume ratio and easy modification, composites based on SiNWs have won a special status in the wide application fields. In this review, we summarize the essential aspects of catalytic activities based on SiNWs. An up-to-date overview of SiNW-based catalysts, including various metal-modified-SiNWs as well as hydrogen terminated SiNWs are discussed in detail. In addition, surface doping effect is illustrated to promote the understanding of catalytic activity.

1 Introduction

Nanosized metal catalysts have attracted various attentions because they can completely degrade many hazardous pollutants through redox processes [1–3]. Although non-supported noble metals have been reported, the metal nanoparticles (NPs) supported by semiconductors or other materials have been considered as a more efficient route when being utilized as heterogeneous catalysts [4, 5].

In recent years, silicon nanowires (SiNWs) were chosen to be one of the supports because of their large surface-to-volume ratio, affinity to environment, and good biocompatible properties. SiNWs were first synthesized by Wagner and Ellis in 1964 via vapor-liquid-solid growth [6]. Since then, SiNWs as one of the most important 1D semiconductors have gained growing concerns due to the central role of Si in the semiconductor industry, and applications in solar cells, sensors, lithium batteries and catalysts [7–12]. Numerous methods, such as laser ablation method [7], thermal-evaporation oxide-assisted growth [10, 12, 13], supercritical fluid solution-phase approach [14], electrodeless etched routes [15] have been investigated to prepare SiNWs, effectively guaranteeing the yields and demands of applications in catalysts.

Each SiNW consists of a crystalline Si core and an outer layer of Si oxide [16], of which the thickness is 1/4–1/3 of the nominal diameter [17]. Therefore, three sections of a SiNW for use should be taken into account: SiNW core, surface passivants, and adsorbates or interface compounds. The large surface-to-volume ratio of SiNWs significantly influence their transport properties, making it possible to modulate the conductivity, catalytic activity and other surface-dependent properties of SiNWs via surface effects.

The Si–O bonds on the surface of SiNWs can be easily converted to Si–H bonds by HF treatment. Due to the reducibility of Si–H bonds, metals such as gold, silver, copper and bimetals are modified on the surface of SiNWs and used in various applications. There are many merits associated with metal-SiNW composites such as favor for reuse, environmental-friendliness and high catalytic efficiency [18, 19]. The composites can avoid agglomeration of metal NPs and increase contact reaction area during the reaction process [20].

In this review, we summarize the essential aspects of catalytic activities based on SiNWs. An up-to-date overview of SiNW-based catalysts, including various metal-

✉ Fan Liao
fliao@suda.edu.cn

✉ Mingwang Shao
mwshao@suda.edu.cn

[1] Jiangsu Key Laboratory for Carbon-Based Functional Materials & Devices, Institute of Functional Nano & Soft Materials (FUNSOM), Soochow University, Suzhou 215123, Jiangsu, China

modified-SiNWs as well as bimetal-modified-SiNWs, is presented here. In addition, the catalytic performance of hydrogen terminated SiNWs are discussed in detail.

2 Catalytic activity of SiNWs

2.1 Metal/SiNWs for catalysis

As mentioned above, the SiNWs are easy to modify with metals. The common method is to etch the as-synthesized SiNWs with proper concentration of HF aqueous solution to form the Si–H bonds, and then rinse them with distilled water and immerse in the metal salt solution. When the yellow SiNWs gradually turn colors, they are modified with metal NPs. SiNWs can assist to absorb UV, visible and even infrared light in the photocatalytic process, capable of greatly increasing the percentage of light energy used. The metals are confirmed to be epitaxial growth on the SiNWs, which are stable and difficult to agglomerate. So metal/SiNWs used in catalysis can remain active and be collected for recycling.

2.1.1 PdNPs/SiNWs

Stabilized clusters or colloids of noble metals such as Pd with nanometer-scale dimensions have been of particular interest as catalysts for organic and inorganic reactions [21–24]. However, the problems, such as high cost, toxicity, un-recyclability and sensitivity to oxygen and water, have hampered their industrial applications [25, 26]. Heterogeneous Pd catalysts have been viewed as positive advances over the past decades [27–30]. The unique features, such as large specific surface areas, easy surface modification and easy acquisition in bulk, enable Si nanostructures a promising support for PdNPs.

Hu et al. [31] used the PdNPs/SiNWs catalysts to reduce methylene blue (MB) in the presence of sodium borohydride. Successive UV–visible spectra of the reduction of MB at sodium borohydride concentration of 1×10^{-3} M (Fig. 1, inset) showed that the absorption bands for MB decreased gradually without any changes in shape or position of the peaks, which indicated that the MB was reduced without any other side reactions. The reaction rate with the PdNPs/SiNWs catalysts is 30 times as high as that with unsupported PdNPs. The most important reason for the decrease of the catalytic activity of unsupported PdNPs was the agglomeration of the particles without any carrier during the operation.

Since the PdNPs were supported on SiNWs, the catalysts can be easily recycled and initiate the next reduction after rinsing with distilled water. The stability of the catalyst was also in comparison to polymer-supported PdNPs (PdNPs/Poly) catalysts (Fig. 1b). While the PdNPs/Poly catalysts lost their activities after recycling for five times, the catalytic rate of the PdNPs/SiNWs catalysts only decreased by 20 % when the cyclic time was up to 50. The inactivated PdNWs/Poly catalysts may account for the polymer reuniting to conglomeration in recycling.

The PdNPs/SiNWs catalyst was also employed for the degradation of eosin Y in the presence of sodium borohydride, offering several potential advantages such as rapid reaction rate, high catalytic activity, and re-utilization [32]. It shows stable and good catalytic activity in Heck coupling reaction, which is a versatile method for carbon–carbon bond formation between aryl halides and alkenes in organic synthesis [33–35]. The PdNPs/SiNWs catalysts can be recycled for at least ten successive runs without appreciable loss of catalytic activity [36].

The above results obviously indicate that the catalytic activity and stability of PdNPs/SiNWs catalysts are promising, capable of finding expansive applications in the catalytic field. The SiNWs supported PdNPs are kept from congregating and growing large because they are fixed by the SiNWs, which also makes it possible for PdNPs catalysts to have high efficiency during the reaction and in recycling use.

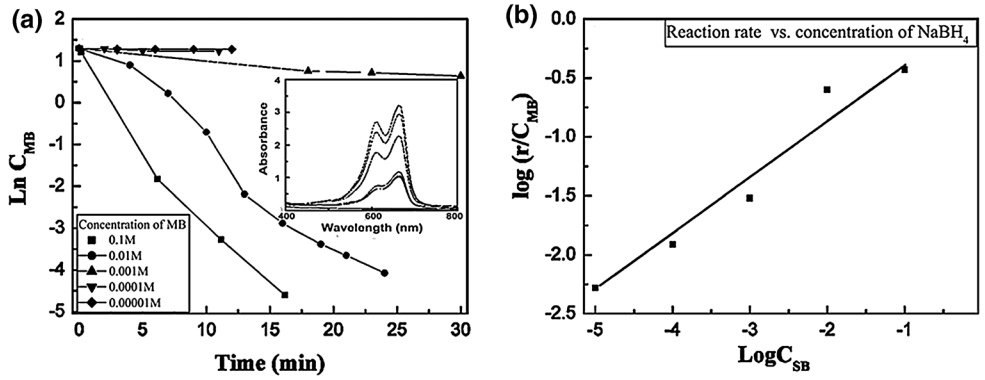

Fig. 1 **a** Curves of concentration versus time at various MB concentrations and successive UV–visible spectra (*inset*) of the reduction of MB at sodium borohydride concentration of 1×10^{-3} M and **b** Curves of MB concentration versus time using PdNPs/SiNWs, unsupported PdNPs, PdNPs/Poly catalysts. Reprinted with permission from Ref. [31]

2.1.2 AuNPs/SiNWs

Nanosized Au particles have attracted much attention in recent years [37, 38], especially their exceptional potential in catalyzing selective epoxidation reactions [39].

Tsang et al. [40] investigated the catalytic activity of AuNPs/SiNWs for oxidation of cis-cyclooctene in the absence of solvent. They found that high conversion efficiency of 38.3 % and high selectivity up to 90 % were achieved simultaneously after 24 h reaction. Details of the conversions and selectivity of cis-cyclooctene oxidation revealed that the percentage of conversion to epoxycyclooctane reached 20 % after 18 h, and the conversion selectivity to epoxycyclooctane maintained at 100 % (Fig. 2). Increasing the oxidation time brought side products, which were composed of a small amount of cycloocten-2-one (7.3 % in total products) and a trace amount of cyclooctanol-2-one (2.7 % in total products). Significantly, the percentage of conversion yielded by present reaction was 4–5 times higher than the previous report (conversion efficiency ~8 %) with the catalyst of AuNPs-supported on graphite (Au/C). At the same time, the selectivity to epoxycyclooctane achieved by AuNPs/SiNWs was up to 90 %, obviously higher than that of 82 % achieved by the AuNPs/C catalyst under the same condition [40]. It should be noted that the AuNPs/SiNWs catalyst with only one-fifth of the total amount of the AuNPs/C catalyst could achieve the present high conversion efficiency and high selectivity.

AuNPs can be stabilized or anchored on SiNWs, and isolated or separated from one another are the main reason for the enhanced catalytic activity of AuNPs/SiNWs.

2.1.3 CuNPs/SiNWs

Cu can take part in cross-coupling chemistry in a way strikingly similar to Pd [41], with much lower cost than Au or Pd. Figure 3 showed that after 24 h reaction high conversion efficiency of 28.3 % and high selectivity up to 97.6 % to epoxycyclooctane were achieved. After 18 h, the percentage

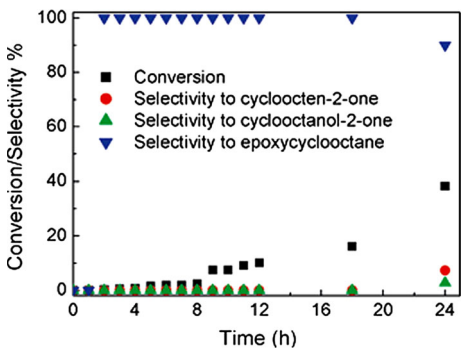

Fig. 2 Reaction profile of Au/SiNWs catalyzed oxidation. Reprinted with permission from Ref. [40]

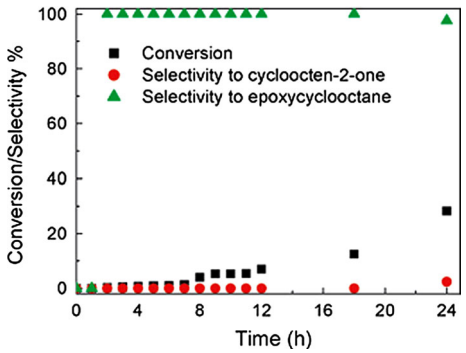

Fig. 3 Reaction profile of CuNPs/SiNWs catalyzed oxidation. Reprinted with permission from Ref. [40]

of conversion to epoxycyclooctane is up to 16 %, and the selectivity to epoxycyclooctane is 100 %. With further oxidation to 24 h, there was only one side product of a trace amount of cycloocten-2-one (2.4 % of total products) detected. Similar to the AuNPs/SiNWs catalyst, the high percentage of conversion and extremely high selectivity may be attributed to the high-density of CuNPs (50 wt% percentage) stabilized on SiNWs, high surface area of CuNPs/SiNWs catalyst, and the unique feature of Si nanostructures.

2.1.4 AgNPs/SiNWs

Ag is one of the most studied metals because of its special properties and numerous applications [42–45]. When the size of Ag particles decreases, their catalytic activity increases due to the large surface-to-volume ratio of AgNPs. Yet, AgNPs are easy to agglomerate during long-time repeated applications. Therefore, SiNWs were used as a substrate to grow AgNPs by Hua et al. [46] and employed as catalysts in the decomposition of fluorescein sodium. The experimental results showed that the decomposition reaction of fluorescein sodium (6×10^{-5} M) using sodium borohydride (1×10^{-5} M) as the reducing agent took place very quickly through the catalysis of AgNPs/SiNWs.

A comparison experiment was carried out with unsupported AgNPs as catalysts. The specific surface area of AgNPs/SiNWs and unsupported AgNPs catalysts were 197.02 $m^2\ g^{-1}$ and 85.64 $m^2\ g^{-1}$, respectively. Owing to one-dimension nanostructure of SiNWs, the AgNPs/SiNWs catalysts are given a large surface-to-volume ratio. The reaction rate of AgNPs/SiNWs enhanced ca. 6 times compared to that of unsupported AgNPs catalysts [46]. These results demonstrated the excellent catalytic activity of silver-modified SiNWs.

2.2 Bimetal/SiNWs for catalysis

Adding a second metallic component in a metal nanostructure has aroused extensive interests because of their

unique optical, electronic, magnetic, and especially catalytic properties. Bimetals can effectively enhance the activity, selectivity, and stability of pure metal catalysts [46, 47]. The improved catalytic performance exhibited by bimetal catalyst is owing to the synergetic effect of the two metals, which requires the two metals being in interaction and in most cases the formation of alloy [48–52]. To prevent bimetallic NPs from aggregation and coalescence which reduces the catalytic activity and surface area, appropriate supports immobilizing bimetallic NPs are widely utilized. Conventional synthesis of bimetallic NP hybrids typically involves simultaneous or successive chemical reduction of two different metal precursors [53–55], which often requires employment of reducing or stabilizing agents, and byproducts are often produced. Modification the SiNWs with bimetals, by contrast, is a facile way to prepare highly efficiency catalysts. The hydrofluoric acid treated SiNWs are simply immersed in the mixture of two metal salt solutions or electroless co-plating the activated SiNWs can obtain the bimetal modified SiNWs [56, 57]. SiNWs could not only stabilize bimetallic NPs but also facilitate electron transfer in catalytic reaction process. The incorporation of bimetallic NPs with SiNWs as a composite is an effective strategy to prepare highly catalysis-active nano-sized hybrids.

2.2.1 *Au–Pd bimetal/SiNWs*

Au–Pd bimetallic catalyst, which is miscible at any ratio as seen in their phase diagram, is one of the most popular systems in catalysis research [58]. Goodman et al. [59] discussed gold's promotional effect in catalysis of Pd–Au via growing Pd catalysts on various Au crystal planes.

Shao et al. synthesized the Au–Pd NPs on the surface of SiNWs and used them in the degradation of the *p*-nitroaniline. The as-prepared catalyst exhibited excellent mutual promotional effect compared with AuNPs/SiNWs and PdNPs/SiNWs catalysts (Fig. 4b). The curves of *p*-nitroaniline concentration versus time using three kinds of catalyst indicated that the reduction rate of Au–Pd/SiNWs catalysts was the highest of the three. This synergistic effect factor was calculated as 2.35. More importantly, the catalytic rate of the catalysts only decreased 20 % after recycling for five times [56].

2.2.2 *Pd–Ni bimetal/SiNWs*

Pd has been extensively used as a good electrocatalyst for ethanol oxidation in an alkaline medium due to the high current density and good stability [60]. It is also more abundant in earth than Pt by about 50 times [21]. Alloying Pd with other metals like Ni could further enhance its catalytic reactivity [61]. Ni is a relatively inexpensive and different metal that have been reported to cope with other metals [61–65].

Miao et al. [57] employed Pd–Ni/SiNWs as an electrocatalyst for ethanol oxidation in alkaline media. The catalytic properties and surface area are important factors in determining the activity of an electrode. The electrochemical active surface (EAS) of the Pd–Ni/SiNWs electrodes is closely related to the surface area and can be measured by determining the Coulombic charge in the reduction of palladium oxide [66]. The Pd–Ni/SiNWs electrode has a larger EAS than that of Pd–Ni/Si, which leads to better dispersion of the catalysts, a larger interface on the Pd–Ni/SiNWs, and higher catalytic activity (Fig. 5). The long-term stability of the electrode was confirmed after 500 cycles, only 12 % loss in the current density is observed from the Pd–Ni/SiNWs electrode.

Besides the good electrocatalytic property of Pd–Ni for ethanol oxidation in alkaline media, the SiNWs supporter also plays an important role: It acts as the backbone of electrocatalyst with high volume to surface ratio and small curvature radii, not only increasing the reaction area but also promoting electron-transfer reactions effective for electrocatalyst. This is important to develop direct ethanol fuel cells. It was the synergistic effect by the interaction among nickel, palladium and SiNWs that made the Pd–Ni/SiNWs nanocomposite have excellent electrooxidation performance to ethanol.

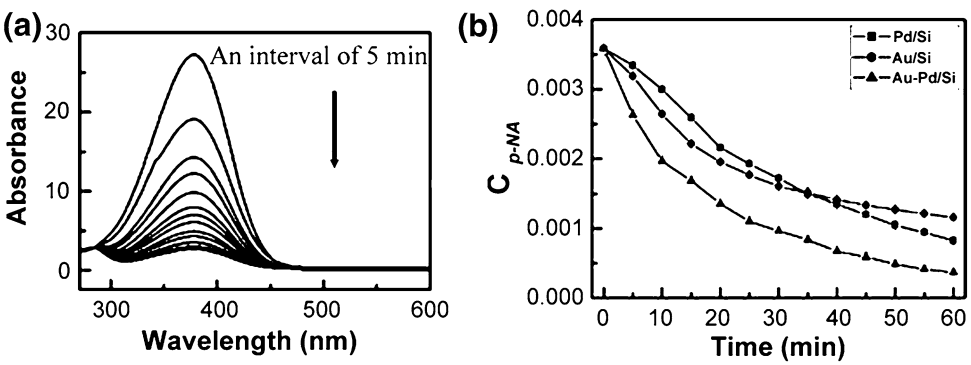

Fig. 4 **a** UV–visible spectra of the degradation of *p*-NA using Au–Pd/Si catalysts and sodium formate as the hydrogen donor. **b** Curves of *p*-NA concentration versus time using Au–Pd/Si, Pd/Si or Au/Si catalysts. Reprinted with permission from Ref. [56]

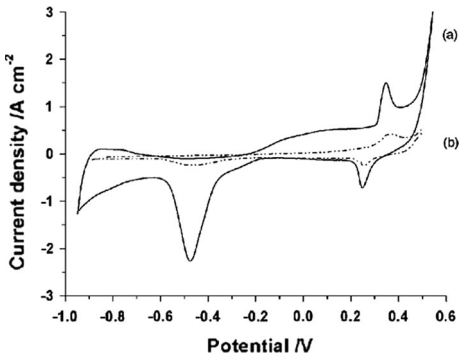

Fig. 5 Cyclic voltammograms of **a** Pd–Ni/SiNWs and **b** Pd–Ni/Si acquired in 1 M KOH solution at room temperature at a scanning rate of 50 mV/s. Reprinted with permission from Ref. [57]

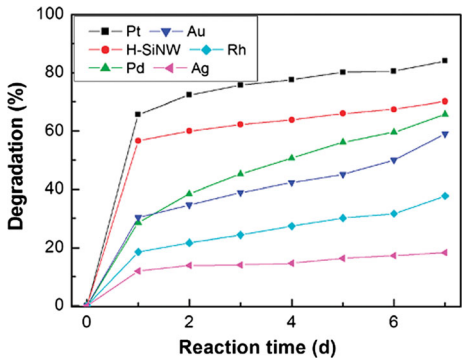

Fig. 6 Degradation of rhodamine B under various SiNW catalysts at different times, which reveals the Pt-modified SiNWs have the best catalytic activity, followed by H-treated, Pd-modified, Au-modified, Rh-modified, and Ag-modified ones. Reprinted with permission from Ref. [67]

2.3 H-terminated SiNWs without modification of metals

In our previous introduction, metals served the decomposition and catalytic oxidation of dyes or small-molecule organic pollutants as the main catalysts while SiNWs play the role of supporter although they can partly enhance the catalytic efficiency. However, as a main group semiconductor, it is interesting to note that SiNWs treated with HF also have catalytic activity. Besides the photo- and ultrasonic oscillations degradation of dyes and small organic molecule, H-SiNWs were found to have catalytic activities similar to those of biological enzymes. Meanwhile, H-SiNWs can also accelerate copper oxidation.

2.3.1 H-terminated SiNWs for photocatalysis

Shao et al. [67] employed HF-treated silicon nanowires (H-SiNWs) as catalysts in the degradation of rhodamine B. To elevate the photocatalytic efficiency of the degradation, noble metal-modified SiNWs were employed, which were generally recognized as effective due to their easy separation of charges with electrons collected in metal particles [68]. However, the results shown in Fig. 6 reveal an unexpected fact: although H-SiNWs were not as good as Pt-modified ones in the photocatalytic activity, they did behave better than Pd-, Au-, Rh-, or Ag-modified ones in the degradation of rhodamine B.

Another unexpected phenomenon was that H-SiNWs maintained excellent photocatalytic activity even though they had been immersed in solution over 1 week. This stability in solution was also critical in the application of silicon materials.

Wang et al. [69] also reported that H-SiNWs were excellent photocatalysts for the decomposition of methyl red under visible light irradiation. Coincidentally, methyl red can be degraded with assistance of H-SiNWs under ultrasonic agitation [70].

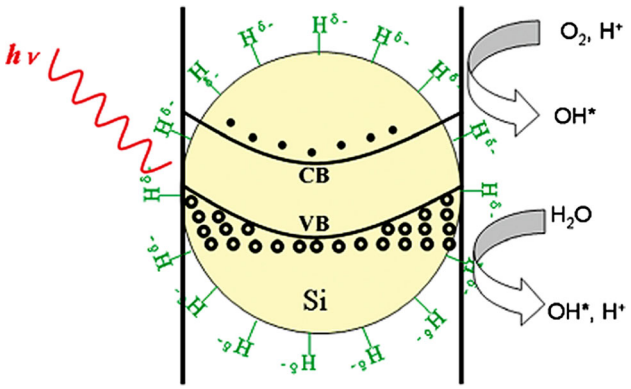

Fig. 7 Schematic of the electron–hole generation in H-SiNW photocatalyst and some of the mechanisms involved: (*left*) Ray promotes the formation of the electron and hole; (*middle*) the electron transfer to hydrogen atom on the surface; (*right*) hole is used in the formation of the OH* groups promoting oxidation processes. Reprinted with permission from Ref. [67]

The mechanism of the photocatalytic activity in metal–semiconductor catalysts lies mainly in the transfer of electron and hole. A noble metal with a high value of electron work function can make the electron transfer process from conducting band to metal more rapidly. This mechanism obviously doesn't match with H-SiNWs.

H-SiNW catalysts' excellent photocatalytic activity may attribute to the hydrogen atoms on the H-SiNW's surface. When a photon with energy equal to or greater than the band gap of the H-SiNW reaches the catalyst's surface, an electron in the conduction band and a hole in the valence band will generate. The induced hole receives the electron from adsorbed water and results in OH* free radical groups (Fig. 7). The terminated hydrogen atom, which has a large Pauling electron negative value of 2.2, with a charge of 0.09–0.13 au may serve as an electron sink and accelerate the separation of the electron and hole, resulting in the

promotion of the photocatalytic efficiency. Finally, the reactive OH* radicals oxidize and degrade adsorbed organic pollutants.

2.3.2 *H-terminated SiNWs for enzyme mimics catalysis*

SiNWs are biocompatible and have a wide range of applications in biomedical research. Wang et al. [71] found that H-SiNWs could reduce MTT [3-(4,5-dimethyl-2-thiazol)-2,5-diphenyl-2H-tetrazolium bromide] in the absence of cells. In the presence of coenzyme, reducing capacity of H-SiNWs was enhanced, thus showing the reductase-like function of SiNWs. They also reported that H-SiNWs have catalytic activities similar to those of biological enzymes catalase and peroxidase [72].

2.3.3 *H-terminated SiNWs for acceleration of copper oxidation*

H-SiNWs not only can serve as excellent photocatalysts, but also act as catalyst to accelerate the oxidation rate of copper. Liao et al. [73] have reported that H-SiNWs accelerated the oxidation rate of copper with the enhancement factor of 10,000 via X-ray diffraction semi-quantitative analysis.

The reason of H-SiNWs exhibit excellent activity lies in the particular semiconductor characteristics of them. The adsorbed water molecules would trap electrons from H-SiNWs and react with O_2 as the following half-reaction: $O_2 + 2H_2O + 4e^- = 4OH^-$. Meanwhile, loss of electrons on the surfaces of H-SiNWs would cause surface band bending and lead to the accumulation of excess holes in the valence band, letting H-SiNWs exhibit a *p*-type semiconductor behavior [74]. Copper can easily get positive holes to form copper cation as the following half-reaction: $2Cu + 2OH^- + 2\ h^+ = Cu_2O + H_2O$. According to the conduction band (CB) and the valence band (VB) of Si (−4.05 and −5.17 eV) and the standard electrode potentials of the above half-reactions (−4.87 and −4.11 eV), the offset between CB and O_2/OH^- is −0.82 eV, which ensured electron transport from H-SiNWs to O_2. The barrier between VB and Cu/Cu_2O is −1.06 eV. Such a large negative injection barrier definitely can facilitate hole injection from H-SiNWs into copper (Fig. 8). Therefore, a faster oxidation occurred and Cu_2O was obtained.

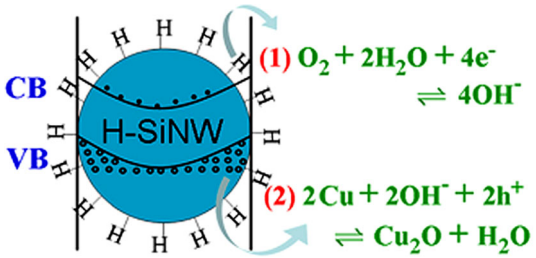

Fig. 8 Schematic of the oxidation process by H-SiNWs. Reprinted with permission from Ref. [73]

3 Surface doping effects of SiNWs

When considering the mechanism of H-SiNWs as catalysts, particular attention has always focused on the surface effects caused by large surface-to-volume ratio. The catalysis of H-SiNWs turned out not to realize in the bulk Si, such as H-terminated Si wafer. In general, extending to nanomaterials, the surface characteristics, such as composition, dangling bonds, and surface states/defects, of nanostructures play a dominant role in determining the materials properties [75]. When the catalytic oxidation of H-SiNWs was illustrated, we mentioned H-SiNWs exhibited a *p*-type semiconductor behavior due to surface doping effect caused by the adsorbed water molecules. This effect is discussed in details below to promote understanding of the surface effect.

Jie has found that the conductance of SiNWs fabricated via chemical etching of *p*-type Si wafer is substantively different in air from that of the original wafer [74]. A hole concentration of a SiNW in field-effect transistors (FETs) is two orders of magnitude higher than that of the original wafer from which the SiNW was etched in air. In vacuum, the hole concentration enhances, which results in the decrease of the conductivity of SiNWs, whereas the hole mobility increases. By embedding SiNW FETs in SiO_2, the device performances show at least one order of magnitude larger than that of the uncoated devices, due to the effects of SiO_2 in insulating the device from atmosphere and passivating the surface defects of nanowires. Owing to the dominant surface effects, *n*-type SiNWs can even exhibit *p*-type characteristics. This interesting phenomenon demonstrates that surface states can dominate the transport properties of SiNWs, and that appropriate surface passivation can significantly improve the performance of SiNW FETs (see Fig. 9) [76].

The tunable and reversible transition of p^+–p–i–n–n^+ conductance was demonstrated in nominally intrinsic SiNWs, which was described as a core–shell structure, via simply changing surface or shell conditions [76].

The large surface-to-volume ratio of SiNWs provides high-efficiency surface modification. First principle calculations also confirmed the doping effects of SiNWs via surface passivation and adsorbates. Surface effects facilitate the doping of SiNWs by electron transfer across the surface layer, which provides a considerable concentration of majority carriers in SiNWs with surface passivants such as hydrogen [77, 78]. It is believed that the effects may find more applications if used properly.

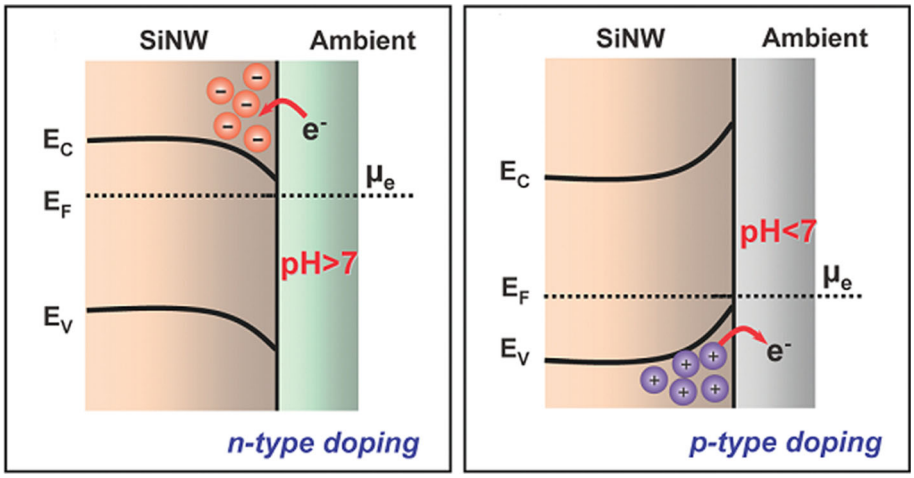

Fig. 9 Schematic of band bending in SiNWs under *n*- and *p*-type doping by electron transfer at the interface between the SiNW and the wet layer. μ_e is chemical potential per electron in the ambient; E_C, E_F and E_V are the conduction band, Fermi energy and valence band of SiNWs, respectively. Reprinted with permission from Ref. [76]

4 Conclusion

In this article, the surface chemical properties and catalytic activities of SiNWs-based materials have been reviewed. SiNWs supported noble metal NPs have exhibited great catalytic activity and have been extensively used in the decomposition of fluorescein sodium, the reduction of MB, coupling reaction and degradation of eosin Y. It should be noted that SiNWs supported bimetal NPs showed excellent synergistic effects in electrooxidation and degradation of the *p*-nitroaniline. The central role of the SiNWs in these catalysts is to anchor the metal NPs and separate from one another to enhance their catalytic activities. The unexpected and unusual results were that H-SiNWs exhibited better photocatalytic activity than most of metal modified ones, and acceleration effect for the oxidation of copper. The surface doping effect contributes to the great performance of the H-SiNWs in catalytic fields and may find more applications in other fields.

Acknowledgments The project was supported by the National Basic Research Program of China (973 Program) (Grant No. 2012CB932903), Major Research Plan of National Natural Science Foundation of China (No. 91433111), Qing Lan Project, Collaborative Innovation Center of Suzhou Nano Science and Technology, Innovative Research Teams of Jiangsu Higher Education Institutions and the Priority Academic Program Development of Jiangsu Higher Education.

References

1. Y.N. Xia, Y.J. Xiong, B. Lim, S.E. Skrabalak, Angew. Chem. Int. Ed. **48**, 60 (2009)
2. N. Tian, Z.Y. Zhou, S.G. Sun, Y. Ding, Z.L. Wang, Science **316**, 732 (2007)
3. M.S. Yavuz, Y.Y. Cheng, J.Y. Chen, C.M. Cobley, Q. Zhang, M. Rycenga, J.W. Xie, C. Kim, K.H. Song, A.G. Schwartz, L.V. Wang, Y.N. Xia, Nat. Mater. **8**, 935 (2009)
4. B. Wen, J.H. Ma, C.C. Chen, W.H. Ma, H.Y. Zhu, J.C. Zhao, Sci. China Chem. **54**, 887 (2011)
5. Q. Shao, R.H. Que, M.W. Shao, L. Cheng, S.T. Lee, Adv. Funct. Mater. **22**, 2067 (2012)
6. R.S. Wagner, W.C. Ellis, Appl. Phys. Lett. **4**, 89 (1964)
7. A.M. Morales, C.M. Lieber, Science **279**, 208 (1998)
8. Y.F. Zhang, Y.H. Tang, N. Wang, D.P. Yu, C.S. Lee, I. Bello, S.T. Lee, Appl. Phys. Lett. **72**, 1835 (1998)
9. Y. Cui, C.M. Lieber, Science **291**, 851 (2001)
10. D.D.D. Ma, C.S. Lee, F.C.K. Au, S.Y. Tong, S.T. Lee, Science **299**, 1874 (2003)
11. Y. Huang, X.F. Duan, Y. Cui, L.J. Lauhon, K.H. Kim, C.M. Lieber, Science **294**, 1313 (2001)
12. L.L. Zhu, Q. Cai, F. Liao, M.Q. Sheng, B. Wu, M.W. Shao, Electrochem. Commun. **52**, 29 (2015)
13. R.Q. Zhang, Y. Lifshitz, S.T. Lee, Adv. Mater. **15**, 635 (2003)
14. J.D. Holmes, K.P. Johnston, R.C. Doty, B.A. Korgel, Science **287**, 1471 (2000)
15. K.Q. Peng, Y.J. Yan, S.P. Gao, J. Zhu, Adv. Mater. **14**, 1164 (2002)
16. S.T. Lee, N. Wang, C.S. Lee, Mater. Sci. Eng., A **286**, 16 (2000)
17. X.H. Sun, H.Y. Peng, Y.H. Tang, W.S. Shi, N.B. Wong, C.S. Lee, S.T. Lee, J. Appl. Phys. **89**, 6396 (2001)
18. M.C. Daniel, D. Astruc, Chem. Rev. **104**, 293 (2003)
19. T. Risse, S. Shaikhutdinov, N. Nilius, M. Sterrer, H.J. Freund, Acc. Chem. Res. **41**, 949 (2008)
20. A. Wittstock, V. Zielasek, J. Biener, C.M. Friend, M. Baumer, Science **327**, 319 (2010)
21. N.T.S. Phan, M. Van Der Sluys, C.W. Jones, Adv. Synth. Catal. **348**, 609 (2006)
22. Y. Li, X.Y.M. Hong, D.M. Collard, M.A. El-Sayed, Org. Lett. **15**, 2385 (2000)
23. W.P. Zhou, A. Lewera, R. Larsen, R.I. Masel, P.S. Bagus, A. Wieckowski, J. Phys. Chem. B **110**, 13393 (2006)
24. Y. Li, M.A. El-Sayed, J. Phys. Chem. B **105**, 8938 (2001)
25. C.C. Luo, Y.H. Zhang, Y.G. Wang, J. Mol. Catal. A: Chem. **229**, 7 (2005)
26. D. Astruc, Inorg. Chem. **46**, 1884 (2007)
27. M.T. Reetz, E. Westermann, Angew. Chem. Int. Ed. **39**, 165 (2000)
28. A. Biffis, M. Zecca, M. Basato, J. Mol. Catal. A: Chem. **173**, 249 (2001)
29. M.J. Jin, D.H. Lee, Angew. Chem. Int. Ed. **48**, 1 (2009)
30. M. Lamblin, L. Nassar-Hardy, J.C. Hierso, E. Fouquet, F.X. Felpin, Adv. Synth. Catal. **352**, 33 (2010)
31. H. Hu, M.W. Shao, W. Zhang, L. Lu, H. Wang, S. Wang, J. Phys. Chem. C **111**, 3467 (2007)
32. F.X. Wang, M.W. Shao, L. Cheng, D. Chen, Y. Fu, D.D.D. Ma, Mater. Res. Bull. **44**, 126 (2009)

33. R.F. Heck, Acc. Chem. Res. **12**, 146 (1979)
34. A.B. Dounay, L.E. Overman, Chem. Rev. **103**, 2945 (2003)
35. W. Zhang, H.L. Qi, L.S. Li, X. Wang, J. Chen, K.S. Peng, Z.H. Wang, Green Chem. **11**, 1194 (2009)
36. L. Liu, M.W. Shao, X.H. Wang, Asian J. Chem. **23**, 3059 (2011)
37. S.J. Zhuo, M.W. Shao, H.Y. Xu, T. Chen, D.D.D. Ma, S.T. Lee, J. Mater. Sci.: Mater. Electron. **24**, 324 (2013)
38. H.J. Yu, X.T. Li, H. Fang, Q.Y. Chen, F. Jiang, G. Shao, J. Mater. Sci.: Mater. Electron. **22**, 690 (2011)
39. M.D. Hughes, Y.J. Xu, P. Jenkins, P. McMorn, P. Landon, D.I. Enache, A.F. Carley, G.A. Attard, G.J. Hutchings, F. King, E.H. Stitt, P. Johnston, K. Griffin, C.J. Kiely, Nature **437**, 1132 (2005)
40. C.H.A. Tsang, Y. Liu, Z.H. Kang, D.D.D. Ma, N.B. Wong, S.T. Lee, Chem. Commun., 5829 (2009)
41. I.P. Beletskaya, A.V. Cheprakov, Coord. Chem. Rev. **248**, 2337 (2004)
42. C. Xue, X. Chen, S.J. Hurst, C.A. Mirkin, Adv. Mater. **19**, 4071 (2007)
43. S. Jiguet, A. Bertsch, H. Hofmann, P. Renaud, Adv. Eng. Mater. **6**, 719 (2004)
44. S. Glaus, G. Calzaferri, R. Hoffmann, Chem. Eur. J. **8**, 1794 (2002)
45. M.W. Shao, M.L. Zhang, N.B. Wong, D.D.D. Ma, H. Wang, W.W. Chen, S.T. Lee, Appl. Phys. Lett. **93**, 233118 (2008)
46. J. Hua, M.W. Shao, L. Cheng, X.H. Wang, Y. Fu, D.D.D. Ma, J. Phys. Chem. Solids **70**, 192 (2009)
47. Y. Xiang, X. Wu, D. Liu, X. Jiang, X. Chu, Z. Li, L. Ma, W. Zhou, S.S. Xie, Nano Lett. **6**, 2290 (2006)
48. Z.J. Wang, C.X. Wang, S.Q. Chen, Y. Liu, Int. J. Hydrogen Energy **39**, 5644 (2014)
49. C.H. Liu, X.Q. Chen, Y.F. Hu, T.K. Sham, Q.J. Sun, J.B. Chang, X. Gao, X.H. Sun, S.D. Wang, A.C.S. Appl, Mater. Interfaces **5**, 5072 (2013)
50. L. Kesavan, R. Tiruvalam, M.H.A. Rahim, M.I.B. Saiman, D.I. Enache, R.L. Jenkins, N. Dimitrators, J.A. Lopez-Sanchez, S.H. Taylor, D.W. Knight, C.J. Kiely, G.J. Hutchings, Science **331**, 195 (2011)
51. R.G. Chaudhuri, S. Paria, Chem. Rev. **112**, 2373 (2012)
52. R. Ferrando, J. Jellinek, R.L. Johnston, Chem. Rev. **108**, 845 (2008)
53. C.V. Rao, C.R. Cabrera, Y. Ishikawa, J. Phys. Chem. C **115**, 21963 (2011)
54. S.J. Guo, S.J. Dong, E.K. Wang, ACS Nano **4**, 547 (2010)
55. J. Chai, F.H. Li, Y.W. Hu, Q.X. Zhang, D.X. Han, L.J. Niu, Mater. Chem. **21**, 17922 (2011)
56. M.W. Shao, H. Wang, M.L. Zhang, D.D.D. Ma, S.T. Lee, Appl. Phys. Lett. **93**, 243110 (2008)
57. F.J. Miao, B.R. Tao, P.K. Chu, Dalton Trans. **41**, 5055 (2012)
58. T.B. Massalski, H. Okamoto, P.R. Subramanian, L. Kacprzak, *Binary alloy phase diagrams* (ASM International, Materials Park, 1990)
59. M.S. Chen, D. Kumar, C.W. Yi, D.W. Goodman, Science **310**, 291 (2005)
60. P.K. Shen, C.W. Xu, Electrochem. Commun. **8**, 184 (2006)
61. O. Savadogo, K. Lee, K. Oishi, S. Mitsushima, N. Kamiya, K.I. Ota, Electrochem. Commun. **6**, 105 (2004)
62. Z. Qi, H. Geng, X. Wang, C. Zhao, H. Ji, C. Zhang, J. Xu, Z. Zhang, J. Power Sources **196**, 5823 (2011)
63. F. Miao, B. Tao, L. Sun, T. Liu, J. You, L. Wang, P.K. Chu, J. Power Sources **195**, 146 (2010)
64. R.N. Singh, A.A. Singh, Int. J. Hydrog. Energy **34**, 2052 (2009)
65. K.S. Kumar, P. Haridoss, S.K. Seshadri, Surf. Coat. Technol. **202**, 1764 (2008)
66. C.W. Xu, P.K. Shen, Chem. Commun., 2238 (2004)
67. M.W. Shao, L. Cheng, X.H. Zhang, D.D.D. Ma, S.T. Lee, J. Am. Chem. Soc. **131**, 17738 (2009)
68. P.V. Kamat, Pure Appl. Chem. **74**, 1693 (2002)
69. F.Y. Wang, Q.D. Yang, G. Xu, N.Y. Lei, Y.K. Tsang, N.B. Wong, J.C. Ho, Nanoscale **3**, 3269 (2011)
70. Z.H. Chen, Y.B. Tang, Y. Liu, Z.H. Kang, X.J. Zhang, X. Fan, C.S. Lee, I. Bello, W.J. Zhang, S.T. Lee, J. Appl. Phys. **105**, 034307 (2009)
71. H.W. Wang, W.W. Jiang, L. Yuan, L. Wang, H. Chen, A.C.S. Appl, Mater. Interfaces **2013**, 5 (1800)
72. H.W. Wang, W.W. Jiang, Y.W. Wang, X.L. Liu, J.L. Yao, L. Yuan, Z.Q. Wu, D. Li, B. Song, H. Chen, Langmuir **29**, 3 (2013)
73. F. Liao, S.S. Liu, M.W. Shao, S.T. Lee, Appl. Phys. Lett. **100**, 093114 (2012)
74. J.S. Jie, W.J. Zhang, K.Q. Peng, G.D. Yuan, C.S. Lee, S.T. Lee, Adv. Funct. Mater. **18**, 3251 (2008)
75. S.S. Liu, F. Hu, J. Zhang, H.X. Tang, M.W. Shao, ACS Appl. Mater. Interfaces **5**, 3208 (2013)
76. G.D. Yuan, Y.B. Zhou, C.S. Guo, W.J. Zhang, Y.B. Tang, Y.Q. Li, Z.H. Chen, Z.B. He, X.J. Zhang, P.F. Wang, I. Bello, R.Q. Zhang, C.S. Lee, S.T. Lee, ACS Nano **4**, 3045 (2010)
77. F. Liao, L. Cheng, J. Li, M.W. Shao, Z.H. Wang, S.T. Lee, J. Mater. Chem. C **1**, 1628 (2013)
78. C.S. Guo, L.B. Luo, G.D. Yuan, X.B. Yang, R.Q. Zhang, W.J. Zhang, S.T. Lee, Angew. Chem. Int. Ed. **48**, 9896 (2009)